A STEAM-EPI Sequence for High Resolution Diffusion-Weighted Imaging at High Field

K. Shmueli[1], D. L. Thomas[1], R. J. Ordidge[1]

[1]Wellcome Trust High Field MR Research Laboratory, Department of Medical Physics and Bioengineering, University College London, London, United Kingdom

Introduction: At high magnetic fields the commonly-used diffusion-weighted imaging technique of spin-echo EPI suffers from susceptibility artifacts which cause geometric distortion and signal drop-out. This means that whole-brain DWI and DTI are likely to suffer from inaccuracies due to artifacts in some regions. It is desirable to reduce the vulnerability of DWI at high field to such artifacts and also to increase the resolution to take advantage of the greater signal available at high field. Here we propose a technique to give high-resolution diffusion-weighted images of a cuboidal region. Selection of a cuboid allows a reduction of the phase encode FOV which therefore allows a trade-off between higher resolution and total echo train length which can be decreased to reduce susceptibility artifacts. The diffusion weighting gradients only have to be applied once for the whole set of slices within the selected cuboid. In this way the gradient 'on' time is reduced in comparison with other 'single-shot' diffusion-weighted techniques such as ZOOM-EPI [**1,2**], STEAM-FLASH [**3**] and DW-RARE [**4**]. A further advantage of this technique over the ZOOM-EPI technique is that the slices can be much closer together. The STEAM-EPI sequence should also require much less RF power than the FLASH and RARE techniques. In this work, preliminary experiments are carried out to show that DW-STEAM-EPI is feasible and gives accurate diffusion coefficients. It is hoped that the technique could be used to focus in on specific brain regions in which the higher resolution could allow clarification of fibre crossings in DTI.

Methods: Experiments were carried out on a SMIS MR 5000 4.7T whole-body MR scanner provided by Philips Medical Systems. The phantom was an 8.5cm diameter glass sphere filled with n-dodecane: T_1 = 1160ms and T_2 = 163ms measured at 1.5T and diffusion coefficient 0.75 x 10^{-9} m^2s^{-1} at 17.5°C [**5**]. This substance was chosen since these values are similar to those in normal white matter. All images were acquired in the coronal orientation.

A standard Stejskal-Tanner diffusion-weighted spin-echo sequence was used to acquire single-slice diffusion-weighted images at 10 b-values from 0 to 1102 $s.mm^{-2}$. The experiment was repeated with the diffusion gradients in each of the X, Y and Z directions. In all cases the apparent diffusion coefficient (ADC) was calculated from a straight-line fit through a graph of ln(mean MR signal inside rectangular ROI) against b.

The DW-STEAM-EPI sequence used is shown in **Figure 1** with parameters TE_{SE} = 70ms, TE = 46ms, TM = 10ms, Δ = 44.88ms, δ = 10ms, FOV = 162x128mm (read x phase) and matrix size = 64x64, acquired with a sinusoidal read gradient and Fourier transformed to 128x128 points. Twelve slices could be prepared and acquired in 594ms, TR = 3000ms. Here the first 90° pulse of a standard STEAM-EPI [**6**] is replaced with a SE diffusion preparation module allowing a faster slice acquisition rate since the minimum STEAM TE is then only limited by the EPI readout module. All the DW-STEAM-EPI images were acquired at 11 b-values from 0 to 1177 $s.mm^{-2}$. Firstly, unprepared images were acquired in which the diffusion preparation module was switched off. The DW-STEAM-EPI sequence was then used to acquire single-slice diffusion-weighted images of a 40x40x2mm cuboid (with diffusion gradients in the X and Y directions). Multislice diffusion-weighted images (12 slices, 2mm slice thickness, 4mm slice centre-centre separation, 40x40x46mm cuboid) were acquired with diffusion weighting gradients in the Z direction. The temperature in the scanner room was measured with a mercury thermometer.

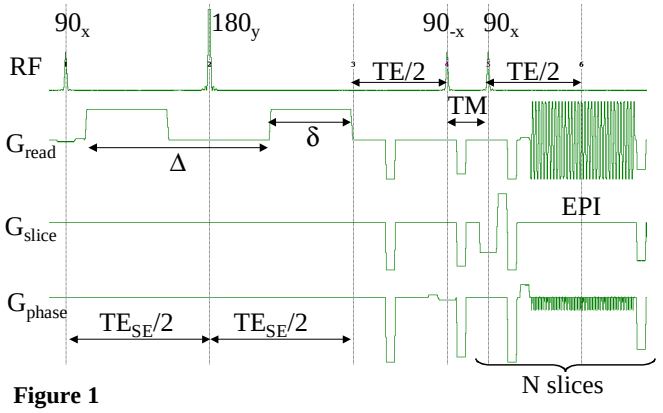

Figure 1

Results: In all cases the r^2 values for the ADC linear fits were greater than 0.95. The temperature in the scanner room was 17.5 ± 1°C.

Figure 2 shows ADC values (left-hand scale) measured with the multislice DW-STEAM-EPI technique (± SD) compared to that measured with the SE sequence (with 95% confidence interval – dotted lines) with the diffusion gradients in the same (Z) direction. The non-diffusion-weighted MR signal values for each DW-STEAM-EPI slice are also included, with an exponential curve fit (right-hand scale). SE ADCs with Y and X diffusion gradients were 0.821 ± 0.014 x 10^{-9} m^2s^{-1} and 0.781 ± 0.009 x 10^{-9} m^2s^{-1} respectively. Single-slice DW-STEAM-EPI ADCs with Y and X diffusion gradients were 0.775 ± 0.012 x 10^{-9} m^2s^{-1} (16 averages) and 0.754 ± 0.012 x 10^{-9} m^2s^{-1} respectively.

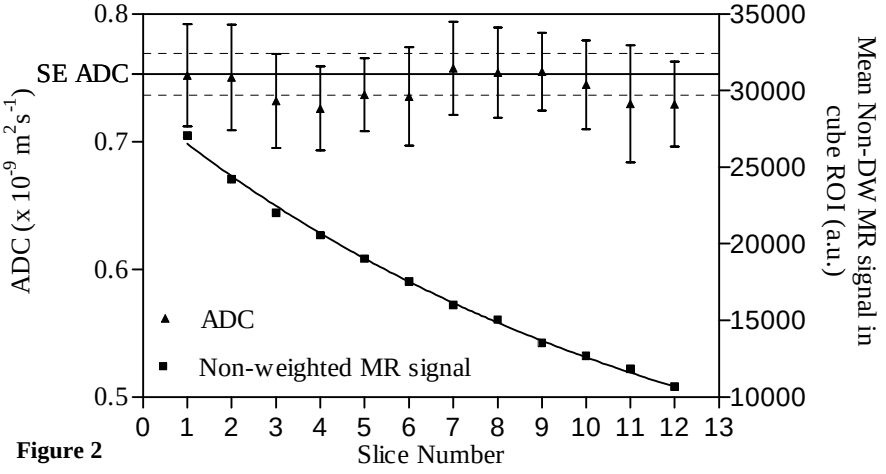

Figure 2

Discussion and Conclusions: The ADC values measured with the multislice and single-slice DW-STEAM-EPI sequence agree with those measured using the standard SE sequence as well as with the literature value above [**5**]. There is no obvious variation in ADC with slice number despite an exponential signal variation caused by T_1 relaxation during the mixing time TM, which increases with slice number. This T_1-related decay might suggest that the SNR in later slices would be severely reduced and give imprecise ADC values. However Figure 2 shows that there is still sufficient SNR after 12 slices to give accurate ADC values. Methods which could increase the overall SNR include slice reversal so that successive averages would have slices acquired in opposite directions. The STEAM technique relies on stimulated echoes, so that there is a factor of 2 SNR penalty compared with a pure SE technique. However this is outweighed by the advantages of the SE diffusion preparation module being decoupled from the readout and the storage of the prepared magnetisation along the Z-axis, so that multiple slices can be acquired while there is still plenty of signal.

References:

1. M. Symms et al, Proc. ISMRM 8:160 (2000)
2. C.A.M. Wheeler-Kingshott et al, MRM 47:24-31 (2002)
3. U.G. Nolte et al, MRM 44:731-736 (2000)
4. K.A. Il'yasov, J. Hennig, JMRI 8:1296-1305 (1998)
5. P.S. Tofts et al, MRM 43:368-374 (2000)
6. R. Turner et al, MRM 14:401-408 (1990)

Acknowledgements: This work is supported by the Wellcome Trust Grant Reference No. 065690